Longitudinal Changes in Retinal Blood Flow in a Feline Retinal Vein Occlusion Model as Measured by Doppler Optical Coherence Tomography and Optical Coherence Tomography Angiography

Takanari Wada, Youngseok Song, Tsuneaki Oomae, Kenji Sogawa, Takafumi Yoshioka, Seigo Nakabayashi, Kengo Takahashi, Tomofumi Tani, Akihiro Ishibazawa, Satoshi Ishiko, and Akitoshi Yoshida

Department of Ophthalmology, Asahikawa Medical University, Asahikawa, Japan

Correspondence: Youngseok Song, Department of Ophthalmology, Asahikawa Medical University, Midorigaoka Higashi 2-1-1-1, Asahikawa 078-8510, Japan; ysong@asahikawa-med.ac.jp.

TW and YS contributed equally to the work and are considered equivalent authors.

Received: April 9, 2019
Accepted: December 16, 2019
Published: February 21, 2020

Citation: Wada T, Song Y, Oomae T, et al. Longitudinal changes in retinal blood flow in a feline retinal vein occlusion model as measured by Doppler optical coherence tomography and optical coherence tomography angiography. *Invest Ophthalmol Vis Sci.* 2020;61(2):34. https://doi.org/10.1167/iovs.61.2.34

Purpose. We aimed to observe longitudinal changes in retinal blood flow (RBF) and structural transformations in capillaries using Doppler optical coherence tomography (DOCT) and optical coherence tomography angiography (OCTA) in a feline retinal blood occlusion (RVO) model.

Methods. RVO was induced by argon green laser photocoagulation (PC) in six eyes of six cats. RBF was measured at a first-order retinal artery and vein by a DOCT flowmeter, and structural changes in the capillaries around the occluded vessels (12 × 12 and 3 × 3 mm) were assessed by OCTA before (at baseline); immediately after PC; and on days 1, 4, 7, and 14 thereafter. Systemic and ocular parameters were monitored during the observation period.

Results. There were no significant differences in any systemic or ocular parameters before and after PC. Arterial RBF increased significantly on day 1 (160.6 ± 8.6% vs. baseline, $P < 0.001$) and decreased below baseline after day 1 through 14. Venous RBF decreased immediately after PC (17.4 ± 9.6% vs. baseline, $P = 0.001$) and then gradually increased afterwards, but did not return to baseline. OCTA showed dilatation of retinal venules immediately after PC to day 1. Collateral vessels began to form on day 4, had matured by day 7, and were pruned on day 14, which formed as mature as normal retinal venule diameters.

Conclusions. With increasing arterial RBF within 1 day after inducing RVO, venules gradually expanded to form collateral vessels, suggesting that collateral vessels originate from existing capillary networks, not neovascularization.

Keywords: retinal blood flow, retinal vein occlusion, vessel remodeling, collateral vessel, Doppler optical coherence tomography, optical coherence tomography angiography

Retinal vein occlusion (RVO) is the second most common retinal vascular disorder and an important cause of visual loss.[1,2] RVO is classified into the following three types: central, hemi, and branch retinal vein occlusion (BRVO).[3] The acute phase of BRVO is characterized by flame-shaped retinal hemorrhage and venous dilation and tortuosity in the affected retina, often with macular edema.[4] During the chronic phase, several retinal vascular abnormalities develop, including capillary nonperfusion, capillary dilation, microaneurysms, telangiectatic vessels, and collateral vessels.[5] Although the pathogenesis of RVO is thought to be multifactorial, including compression of the vein at the arteriovenous crossing, degenerative changes in the vessel wall, and abnormal hematological factors,[6] it is still not completely understood.

Evaluation of ocular circulation is of utmost importance for understanding the physiological and pathological features of retinal vascular diseases.[7] Several studies have reported that retinal blood flow (RBF) in areas with BRVO is lower than in healthy human retinas.[8–10] Abnormal vascular changes have also been reported, including microaneurysms, telangiectasia, and retinal capillary nonperfusion.[11–13] However, the dynamic changes in RBF during the pathologic process of RVO and the relationship between RBF and the resulting structural changes in retinal microvasculature have not been well studied because it is not possible to compare RBF before and after the development of RVO unless RBF was measured in the patients for some other reason before RVO development.

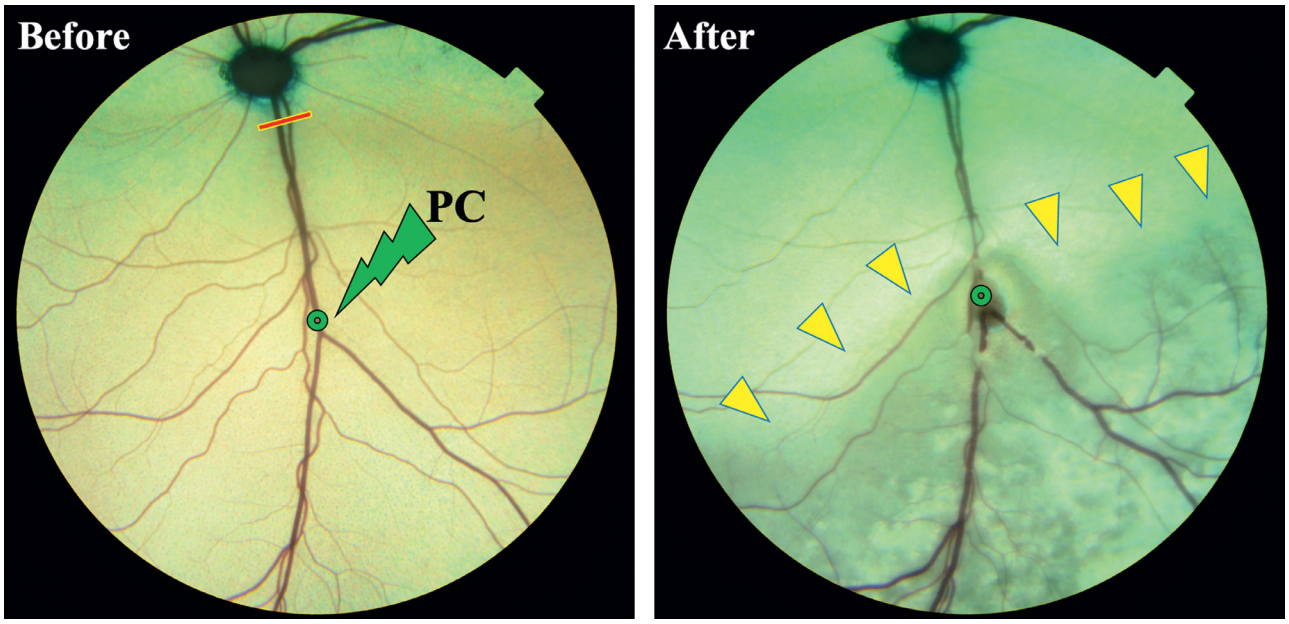

Figure 1. Fundus photo before and after inducing RVO. RBF was measured in the superior branch of the first-order major temporal retinal vessels (*red in yellow bar*). RVO was induced by photocoagulation to the retinal vein at least 1.0 disc diameter away from the optic disc to avoid damaging the adjacent arteries (*green circles*). After RVO induction, retinal edema was observed in the affected perfusion area (*yellow arrowhead*). After, after photocoagulation; before, before photocoagulation; RBF, retinal blood flow; RVO, retinal vein occlusion.

The experimental animal models of RVO, wherein the functional and structural features resemble those of BRVO, can be used to study the pathogenesis of BRVO.[14] The dynamic changes around the induction of occlusion can be demonstrated using the experimental animal models of RVO induced by laser photocoagulation (PC) on a venule.[8,15,16]

Recently, technological devices for measuring RBF have been developed so that it is possible to measure the absolute value of RBF by Doppler optical coherence tomography (DOCT) flowmeter[10,17–19] and noninvasively evaluate the detailed microvascular formations by optical coherence tomography angiography (OCTA).[13,20]

In the present study, we investigated the longitudinal changes in RBF in terms of the functional and microvascular formation changes simultaneously with the structural changes using DOCT and OCTA in a PC-induced feline RVO model.

Materials and Methods

Animal Preparation

The Animal Care Committee of Asahikawa Medical University approved the protocols for the use of animals, which adhered to the Association for Research in Vision and Ophthalmology Statement for the Use of Animals in Ophthalmic and Vision Research. Six adult European shorthair cats provided by Shiraishi Laboratory Animals Co., Ltd. (2.3–3.6 kg; Koshigaya, Saitama, Japan) of either sex were anesthetized with ketamine 5 mg/kg and medetomidine 0.2 mg/kg. The mean arterial blood pressure (MABP) and heart rate were monitored with an oscillometric sphygmomanometer (Vet 20; SunTech Medical, Inc., Morrisville, NC, USA), and the saturation of percutaneous oxygen (SpO_2) was monitored with a pulse oximeter (SurgiVet V1030; Smiths Medical Inc., Minneapolis, MN, USA). The rectal temperature was measured and maintained between 37°C and 38°C with a heated blanket. The pupils were dilated with 0.5% tropicamide (Santen Pharmaceutical Co., Osaka, Japan). A 0-diopter contact lens (Seed Co. Ltd., Tokyo, Japan) was placed on the cornea, which was protected by instillation of a drop of sodium hyaluronate (Healon; Abbott Medical Optics, Inc., Abbott Park, IL, USA). The IOP was measured with a rebound tonometer (Icare TA01i; Icare Finland Oy., Vantaa, Finland) before and after the RBF measurements. The ocular perfusion pressure (OPP) was calculated as OPP = MABP − IOP.[21,22]

Experimental Protocols

RBF and the microvascular formations were measured by DOCT and OCTA before (baseline), immediately after laser PC, and 1, 4, 7, and 14 days after the induction of RVO.

Induction of RVO

RVO was induced using an argon green laser (Novus Omni; Coherent Inc., CA, USA) mounted on a slit lamp. A contact lens (SMT 005 Retina 90 lens; Katena Products, Inc., NJ, USA) was placed on the cornea, and the argon laser was applied to the superior branch of the temporal retinal vein. An occlusion site was selected 1.0 to 3.0 disc diameters away from the edge of the optic disc to avoid damaging the adjacent arteries, because the nearer to the optic disc, the closer the retinal artery and vein (Fig. 1). The laser spot size was 200 μm, the duration was 0.2 seconds, and the power was 300–500 mW as previously described.[23] Thereafter, 20–30 shots were applied on the selected vessel until the vein was observed to be constricted, with the blood cells flowing in the vein stagnated upstream of the occlusion site. The occlusion of the retinal vein had been confirmed with OCTA during the observation period.

Investigative Ophthalmology & Visual Science

RBF Measurements

A DOCT system was used to simultaneously measure the vessel diameter (D), blood velocity (V), and RBF in the superior branch of the first-order major temporal retinal vessels (Fig. 1).

The system is based on a commercially available spectral-domain OCT system (3D OCT-2000; Topcon Corp., Tokyo, Japan) operating at an 800-nm wavelength range.[24] Only the software was modified for blood flow imaging, for which extra image-processing software and quantification software were newly developed to measure blood flow.

The detailed explanation of algorithm measuring retinal blood flow using DOCT was described elsewhere.[24] Briefly, the flow velocity $\upsilon(z)$ can be derived from the Doppler shift incurred by the moving blood:

$$\upsilon(z) = \frac{\Delta\Phi(z,\tau)\cdot\lambda_0}{4\pi\cdot n\cdot\tau}\cdot\frac{1}{\cos\theta} \quad (1)$$

where z is the depth location, $\Delta\Phi$ is the phase difference at the same depth location between the adjacent profiles after Fourier transform, λ_0 is the center wavelength, n is the refractive index of blood, τ is the time interval between the adjacent profiles, and θ is the Doppler angle between the flow vector and the incident probe beam. The blood vessels were detected automatically and identified from the OCT structured and phase images. The vessel diameter also was measured by using OCT phase images. The blood flow rate can be calculated by integrating the velocity in the blood vessel.

Microvascular Formation Imaging

The system used for the OCTA images was OCTA Ratio Analysis (OCTARA) algorithm on a commercially available swept-source OCT device (DRI OCT Triton; Topcon Corp.), which operates at 100,000 A-scans per second, with a 1050-nm wavelength scanning light. OCTARA is based on an intensity ratio analysis; it does not require splitting the spectrum and therefore preserves axial resolution.[25,26] IMAGEnet 6 software was used for imaging the morphologic alterations in the retinal microvasculature. En face OCTA images of the total retinal vasculature (= superficial + deep-layer slabs), projecting from the internal limiting membrane to the retinal pigment epithelium, were evaluated. A 12 × 12-mm area with a 512 × 512 resolution centered on the occlusion site and a 3 × 3-mm area with a 320 × 320 resolution in the vicinity of the occlusion site, were scanned in all eyes. OCTA images in the total slab but not each slab were shown because we confirmed that the blood flow images in the superficial layer projected to the deep layer because of comparatively strong vessel dilations and engorgements for retinal thickness in a preliminary study.

Observation of the Retinal Thickness

During the observation period, the retinal thicknesses were measured using OCT images (DRI OCT Triton, 12 × 12-mm area with a resolution of 512 × 512). The thicknesses were measured by TW and YS at the following three points: proximal side (optic disc side) of the PC point, adjacent to the PC point, and distal side of the PC point, on both sides of the vein (one disc away from the vein).

Statistical Analysis

All data are expressed as the mean percentage ± standard error of the mean. The changes in RBF were calculated as the percentile change from the baseline measurements. One-way ANOVA was used for repeated measurements, followed by post hoc comparisons with the Dunnett test. Group comparisons of the RBF, retinal thickness, and systemic parameters were performed using the Wilcoxon signed-rank test, and $P < 0.05$ was considered statistically significant.

Results

Changes in Systemic and Ocular Parameters

There were no statistically significant differences in MABP, heart rate, IOP, OPP, or SpO_2 throughout the observation (from baseline to day 14) as assessed by one-way ANOVA (Table 1).

RBF Changes After Induction of RVO

Figure 2 shows the percentile changes in retinal circulation after RVO induction, and Table 2 shows the actual values of the retinal circulation before and after RVO induction. Each retinal circulation data of the six cats is shown in Supplemental Figure. 1. After occlusion, the arterial RBF (aRBF) did not immediately change from the baseline (94.2 ± 13.7%, $P = 0.9767$); however, on day 1, the arterial vessel diameter (aD) and aRBF significantly increased (aD, 120.6 ± 5.3%, $P = 0.04$; aRBF, 160.6 ± 8.6%, $P < 0.001$). Furthermore, the arterial blood velocity (aV) increased from the baseline on day 1 (117.0 ± 6.0%); however, this change did not reach statistical significance ($P = 0.11$). On day 4, aD, aV, and aRBF started to decrease; these values were lower than those at the baseline (aD, 90.6 ± 2.9%; aV, 79.3 ± 3.5%; aRBF, 72.0 ± 6.6%). For the rest of the observation period, these values did not return to the baseline values (Fig. 2A).

The venous vessel diameter (vD), venous blood velocity (vV), and venous RBF (vRBF) significantly decreased immediately after occlusion (vD, 31.8 ± 14.5%, $P = 0.005$; vV, 36.8 ± 17.8%, $P = 0.01$; vRBF, 17.4 ± 9.6%, $P = 0.001$). On day 1, vD and vRBF started to increase (vD, 50.7 ± 22.8%; vRBF, 28.1 ± 15.6%) and did not return to the baseline values for the remaining observation period (vD, 85.6 ± 7.2%; vRBF, 64.4 ± 5.9%). vV further decreased by day 1 (31.3 ± 19.0%), and then started to increase on day 4 (48.5 ± 13.7%); however, similar to the other parameters, vV did not return to the baseline value during the observation period (54.0 ± 26.0%; Fig. 2B).

Microvascular Formation Changes

OCTA showed that the retinal vein started to dilate immediately after PC through day 1 and began to form collateral vessels around the occluded vein leading up to day 4 (Fig. 3). By day 7, the collateral vessels reached maturity, and they were pruned on day 14 to a similar size as the original retinal vein (Fig. 3). In a 3 × 3-mm area, the collateral vessels were found to have formed by dilation of the originally existing capillary networks (Fig. 4), as observed in the retina on the B-scan OCTA image (Fig. 5).

Investigative Ophthalmology & Visual Science

Table 1. Systemic and Ocular Parameters Before and After RVO Induction

	Before	After	Day 1	Day 4	Day7	Day14
MABP, mm Hg	132.2 ± 6.9	127.5 ± 3.3	125.8 ± 5.0	125.8 ± 7.9	126.5 ± 4.5	124.8 ± 4.5
HR, beats/min	118.0 ± 4.6	119.8 ± 2.1	119.7 ± 2.4	115.0 ± 4.1	121.5 ± 3.0	118.3 ± 4.5
SpO2, %	96.2 ± 0.7	97.2 ± 0.7	97.2 ± 0.3	97.5 ± 0.8	97.5 ± 0.7	98.3 ± 0.8
IOP, mm Hg	17.6 ± 0.7	17.1 ± 0.5	17.4 ± 0.5	17.6 ± 0.6	17.4 ± 0.6	17.7 ± 0.5
OPP, mm Hg	114.6 ± 6.6	110.4 ± 3.2	108.4 ± 5.3	108.3 ± 7.7	109.1 ± 4.1	107.1 ± 4.2

Data are expressed as the means ± standard errors of the mean. For the comparison before inducing RVO, we used the Wilcoxon signed-rank test.

$P < 0.05$ was considered statistically significant. We found no significant ($P > 0.05$) differences in any parameters before and after RVO induction. Additionally, we found no statistically significant changes in the systemic and ocular parameters throughout the observation period using one-way ANOVA.

After, after RVO induction; before, before RVO induction; day 1, the next day following RVO induction; HR, heart rate; IOP, intraocular pressure; MABP, mean arterial blood pressure; OPP, ocular perfusion pressure; RVO, retinal vein occlusion; SpO_2, saturation of percutaneous oxygen.

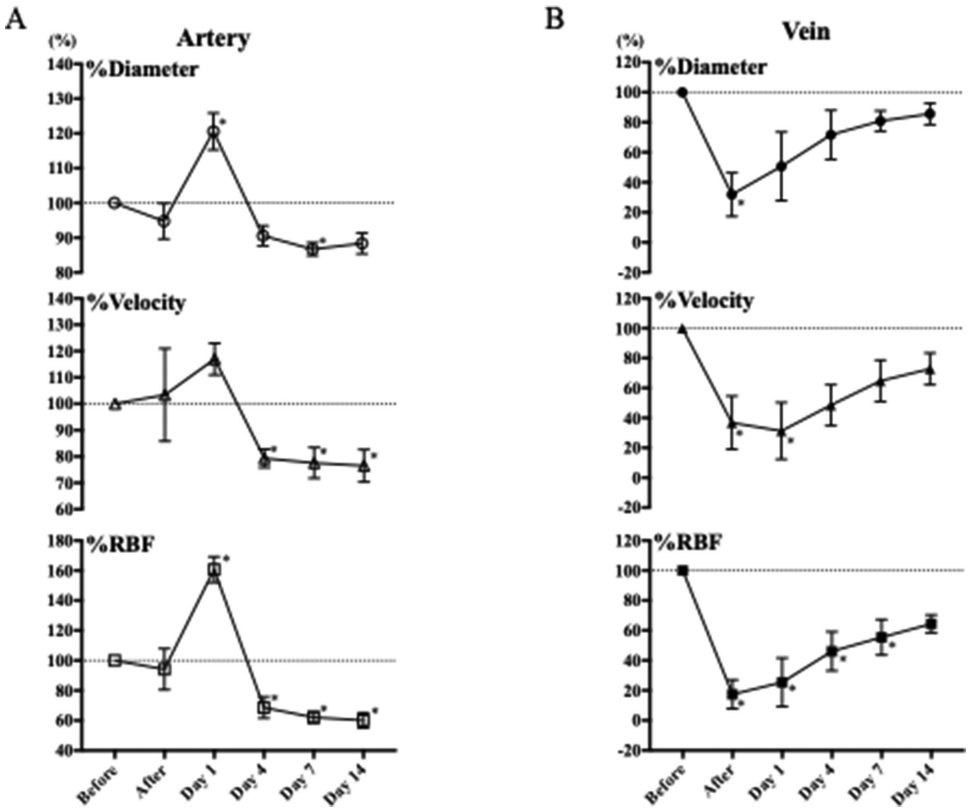

Figure 2. Time course of the changes in retinal circulation. (**A**) On day 1, aD and aRBF significantly increased. On day 4, aD, aV, and aRBF started to decrease. These levels were lower than those at the baseline and did not return to the baseline values. (**B**) vD, vV, and vRBF significantly decreased after the induction of RVO. On day 1, vD and vRBF started to increase. On day 4, vV started to increase but did not return to the baseline. The data are expressed as the mean percentage ± standard errors of the mean of the baseline values. *$P <$ 0.05 compared with the baseline by one-way repeated-measures ANOVA, followed by the Dunnett procedure. aD, arterial vessel diameter; aV, arterial blood velocity; after, after RVO induction; aRBF, arterial retinal blood flow; before, before RVO induction; day 1, the next day following RVO induction; RVO, retinal vein occlusion, vD, venous vessel diameter; vRBF, venous retinal blood flow; vV, venous blood velocity.

Changes in Retinal Thickness

Before the induction of RVO, retinal thicknesses were measured (proximal, 164.9 ± 4.5 µm; adjacent to the PC point, 155.8 ± 4.4 µm; distal, 136.7 ± 3.5 µm). Immediately after the induction of RVO, the thickness at each site significantly increased (177.0 ± 5.2 µm, $P = 0.03$; 174.8 ± 5.6 µm, $P < 0.001$; 163.0 ± 5.6 µm, $P < 0.001$) and remained thicker on day 1 than that before the induction of RVO (177.5 ± 4.5 µm, $P = 0.02$; 181.1 ± 3.4 µm, $P < 0.001$; 165.3 ± 4.0 µm, $P < 0.001$). On day 4, the thickness of each site started to decrease, but remained significantly thick at the distal sites until day 7. On day 14, they returned to the thickness as that before the induction of RVO (163.3 ± 3.7 µm, $P = 0.99$; 154.0 ± 4.6 µm, $P = 0.99$; 138.1 ± 2.9 µm, $P = 0.99$; Fig. 6).

Investigative Ophthalmology & Visual Science

Table 2. The Actual Measurement Values of the Retinal Circulation Before and After RVO Induction

Artery	Before	After
Diameter, μm	105.2 ± 4.0	99.4 ± 5.4
Velocity, mm/s	42.0 ± 3.4	43.0 ± 7.3
RBF, μL/min	17.2 ± 1.9	16.2 ± 3.1
Vein	Before	After
Diameter, μm	138.0 ± 4.8	42.8 ± 19.7*
Velocity, mm/s	20.6 ± 1.2	7.0 ± 3.6*
RBF, μL/min	14.5 ± 1.5	2.4 ± 1.5*

Data are expressed as the means ± standard errors of the mean. For the comparison before inducing RVO, we used the Wilcoxon signed-rank test.

*$P < 0.05$ was considered statistically significant. Arterial RBF did not change immediately after the induction of RVO. The venous vessel diameter, venous blood velocity, and venous RBF decreased significantly immediately after RVO induction. After, after RVO induction; before, before RVO induction; RBF, retinal blood flow; RVO, retinal vein occlusion

Discussion

In this study, a feline RVO model was created by argon green laser PC, and the dynamic changes in RBF were measured using DOCT and OCTA for 14 days. DOCT showed that aRBF increased on day 1 after occlusion and then decreased. vRBF decreased immediately after occlusion and then gradually increased. Interestingly, both arterial and venous RBF never returned to baseline during the observation period. OCTA showed that the collateral vessels formed a "bypass" around the occlusion site after the induction of RVO, indicating that the collateral vessels were formed after dilation of the originally existing capillaries rather than from neovascularization.

The study that comprehensively reviewed animal RVO models has reported that all RVO models revealed early features classically observed in human, including cessation of blood flow and venous dilation, engorgement, and tortuosity distal to the occlusion site.[14] Moreover, the models generally demonstrated retinal hemorrhages and edema, which may make them suitable models to study the acute phase of RVO.[14] In our RVO model, those early characteristic features were found, indicating that our model can be considered suitable to study the acute phase of RVO. The study also reported that most animal models of RVO demonstrated spontaneous reperfusion and/or vascular remodeling, which seemed to occur more rapidly and effectively than in humans with RVO.[14] The period needed for developing collateral vessels to mature was much shorter in our model than that in human eyes,[27] possibly because the animals used for RVO models were young and healthy, whereas patients with RVO are often older and many have underlying systemic disorders, such as hypertension, dyslipidemia, dysfunctional thrombotic responses, or impaired glucose tolerance/diabetes, among others.[14] Because RVO in our animal model was artificially and acutely induced by laser photocoagulation, the process of the condition forming the RVO would be different than clinical cases. Applying disease models such as hypertension and arteriosclerosis with RVO induced by more natural ways may provide clues to the reasons behind these discordances.

In a previous study using a monkey RVO model, which involved the intravenous injection of a radioactive substance, the radiation density was lower in enucleated BRVO model eyes than in healthy eyes 2 hours after occlusion; this reduction in the radiation density lasted until 1 week, implying that RBF may decrease in BRVO eyes.[8] Our findings showed that aRBF increased on day 1, although RBF started to decrease afterwards.

A previous study reported venous collaterals arising from the preexisting capillary bed and an increase in endothelial cell density in capillary vessels in collateral circulation

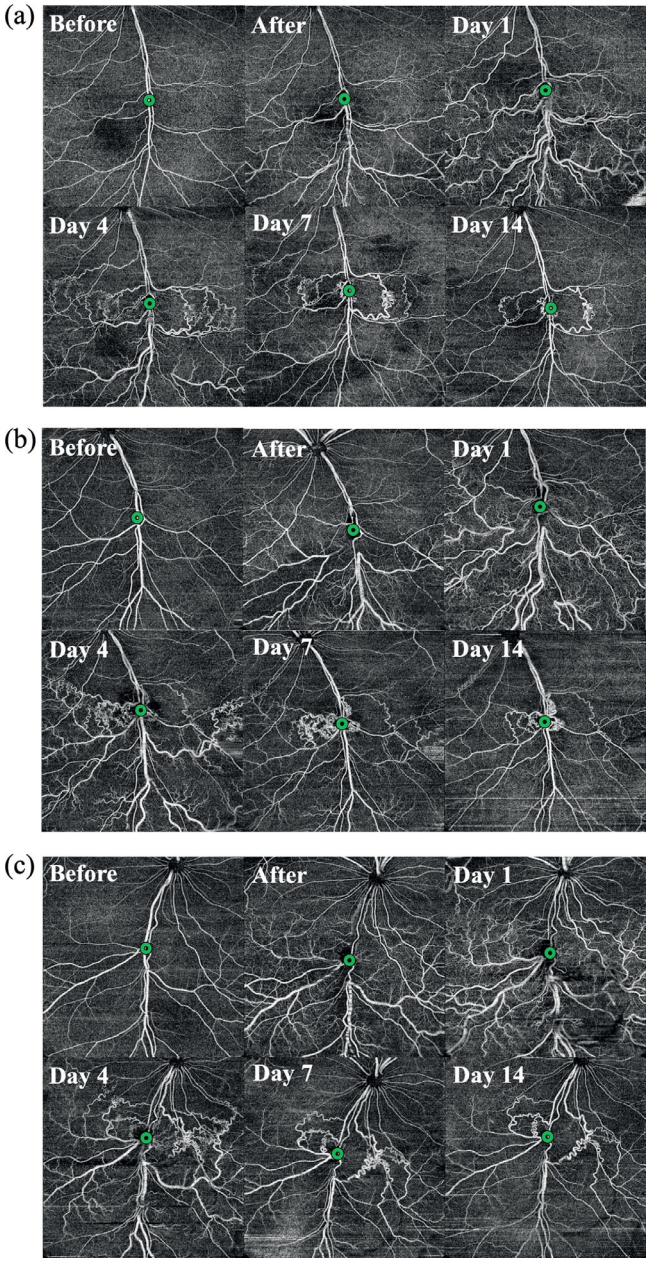

Figure 3. Three representative series of images showing microvascular formation changes as observed using OCTA (12 × 12 mm, total retina slab). The retinal veins started to dilate immediately after photocoagulation through day 1 and began to form collateral vessels leading up to day 4. On day 7, the collateral vessels had reached maturity. On day 14, they had been pruned to a similar size as the original retinal vein. *Green circles* indicate the area where RVO was induced by photocoagulation. After, after RVO induction; before, before RVO induction; day 1, the next day following RVO induction; OCTA, optical coherence tomography angiography.

Investigative Ophthalmology & Visual Science

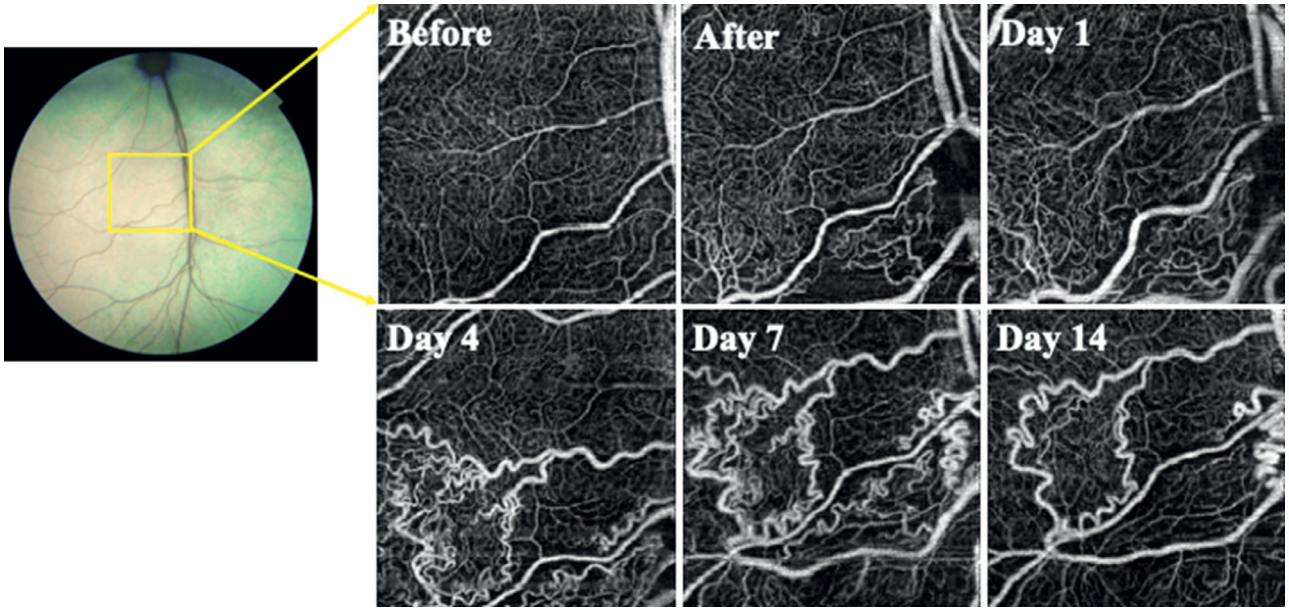

Figure 4. Microvascular formation changes around the occlusion site (3 × 3 mm). The magnified image of the vicinity of the occlusion site was obtained by OCTA of a 3 × 3-mm area (square). The collateral vessels were observed to be formed by dilation of the originally existing capillary networks. *Green circle* indicates the area where RVO was induced by photocoagulation. After, after RVO induction; before, before RVO induction; day 1, the next day following RVO induction; OCTA, optical coherence tomography angiography.

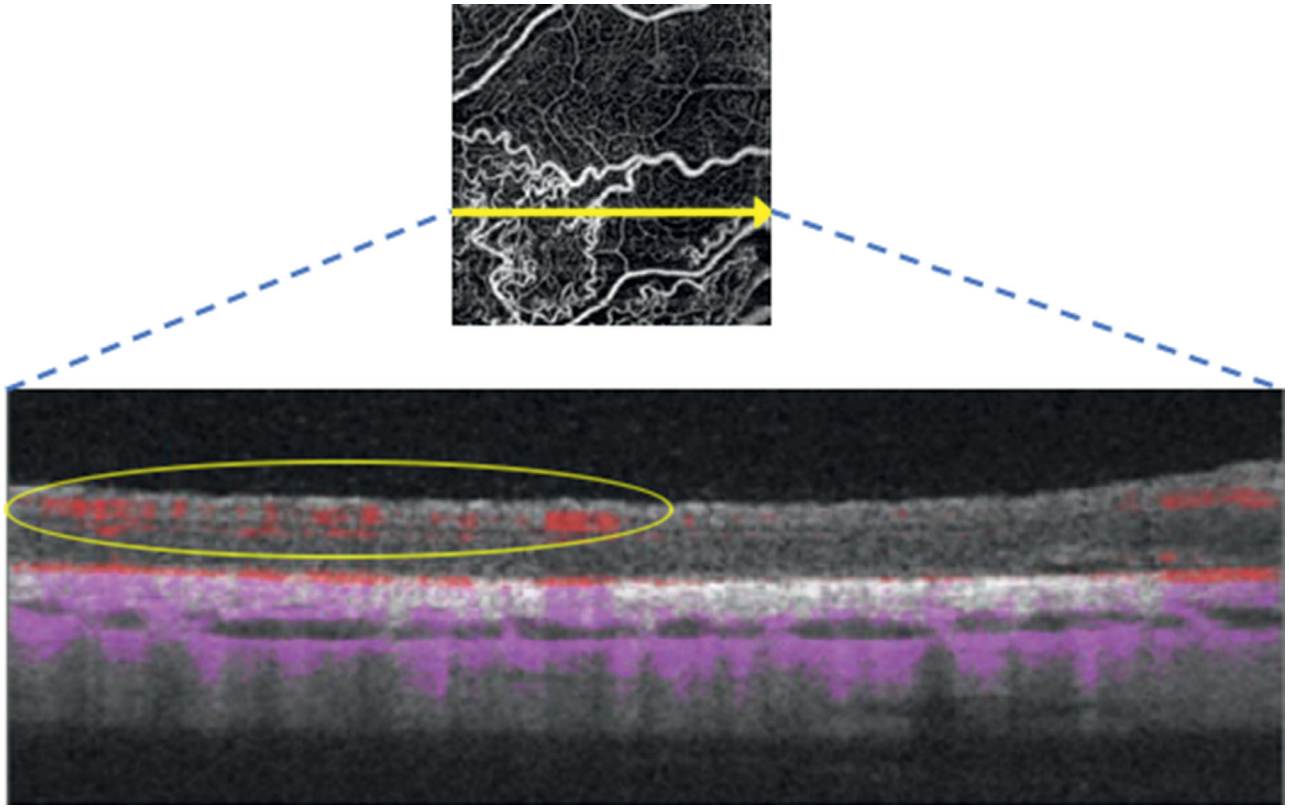

Figure 5. B-scan image of OCTA at the collateral vessels. The blood flow signals are displayed in *red* (above RPE) and in *purple* (below RPE) on the B-scan image (*yellow arrow*). The blood flow signals of the collateral vessels were observed in the retina (*yellow circle*). OCTA, optical coherence tomography angiography; RPE, retinal pigment epithelium.

Investigative Ophthalmology & Visual Science

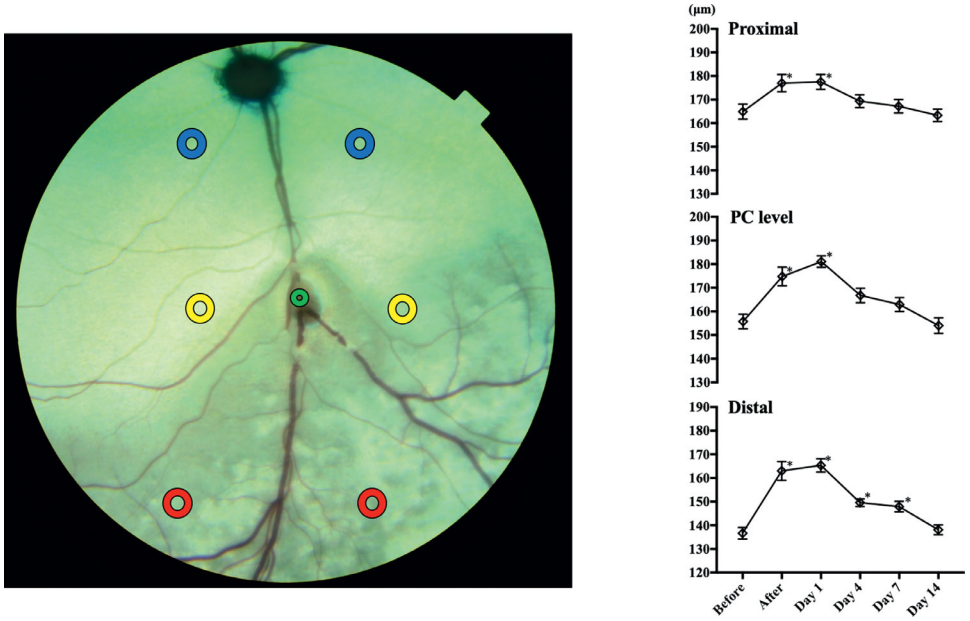

Figure 6. Changes in the retinal thickness. Retinal thicknesses were measured using OCT images at the following sites: proximal of the PC point, PC point level, and distal of the PC point (*blue*, *yellow*, and *red circles*). Immediately after the induction of RVO and on day 1, the thickness of the measured sites significantly increased. On day 4, the thickness of each site started to decrease. On day 14, the thickness returned to the same level as that before the induction of RVO. Green circle indicates the area where RVO was induced by photocoagulation. The data are expressed as mean ± standard errors of the mean. *$P < 0.05$ compared with the baseline by one-way repeated-measures ANOVA, followed by the Dunnett's procedure. After, immediately after the induction of RVO; before, before the induction of RVO; day 1, the next day following the induction of RVO; OCT, optical coherence tomography; PC, photo coagulation; RVO, retinal vein occlusion.

areas.[28] Endothelial cell proliferation in vessels is a feature of neovascularization and may reflect the action of a hypothetical angiogenic factor associated with retinal ischemia.[28] Here, OCTA confirmed that the preexisting capillaries gradually dilate and collateral vessels form after occlusion, which suggests that collateral vessels did not result from neovascularization, but simply by the dilation of preexisting capillaries. This study confirms that collateral vessels are formed after dilation of the preexisting capillaries through advanced imaging technology.

Immediately after the induction of RVO, the retinal thickness of each measured site significantly increased until day 1 (Fig. 6). A previous study of mouse RVO model reported that the retinal thickness dramatically increased within 1 day after the induction of photocoagulation, and then gradually recovered and returned to the baseline.[29] That study showed that the expression of VEGF-A in the retina increased 12 hours after photocoagulation and intravitreal administration of anti-VEGF antibody suppressed the increase in cystoid edema.[29] In this study, the retinal thickness and aRBF peaked on day 1, and the former started to decrease from day 4. Therefore, those bioactive substances might affect aRBF and the retinal thickness. Our preliminary study showed no significant difference in aRBF before and after the induction of peripheral PC (data not shown). This suggests that the effect of PC on retinal edema should be minimal. A previous report speculates that retinal edema is closely related to increased retinal arterial blood flow because of microvascular dilatation by NO[30] and increased permeability by VEGF and other bioactive substances.[31] It is also speculated that aRBF increases on clinical occurrence of retinal edema.[32]

The present study has some limitations. First, the RVO model involved complete and rapid artificial occlusion by exposing the retinal vein to PC, and may not correspond to the actual condition of RVO in clinical practice. Besides, the bioactive substances affecting retinal blood flow such as NO and VEGF levels in the vitreous were not measured, hence the precise mechanisms of the hemodynamic changes are still unknown. Further animal studies with blocking NO and VEGF are expected to confirm if these agents are related to the changes in RBF and collateral formation in RVO. Second, although no obvious neovascularization was observed, it is difficult to confirm whether it occurred at the histological level because of the quality of the OCTA resolution. Third, there were a few cases that did not seem to have complete RVO. The absence of OCTA signals at the location of the laser indicates completeness of the occlusion despite of vRBF remaining at the optic nerve head side of the occlusion. Those that venous blood flow remains at the DOCT measurement site have venous branches between the occlusion site and the measurement site (Supplemental Figs. S2a, b, d). On the other hand, venous blood flow is zero (below the detection limit) at the DOCT measurement site for those having the blood vessel running with small and few venous branches (Supplemental Figs. S2c, e, f). In other words, individuals whose venous blood flow cannot be detected at the measurement site have few vein branches between the occlusion site and the measurement site, and their arteriovenous vessel running is far from being affected by the PC. Studying individuals with such specific conditions would provide further insight into the mechanisms of RVO. Fourth, it seems that aRBF increased and retinal vessels started to dilate, and decreased once collateral vessels started to form. We hypothesized that the gap in RBF between the arteries and veins after occlusion dilated the capillary network physically and physiologically, resulting in collateral vessel formation. However, the causal relationship between them is unclear and requires further

studies. Further, because our observation period was relatively short (~14 days), any changes in this RVO model during the chronic phase remain unclear, including conditions seen in clinical practice such as sheathed (white) retinal veins and nonperfusion area. Further studies with a longer follow-up are needed.

We created a feline RVO model with argon laser PC at the retinal vein. From the longitudinal observation around the induction of RVO, we revealed that aRBF increased on day 1 after occlusion and then decreased. vRBF decreased immediately after occlusion and gradually increased on day 1 and thereafter; however, RBF eventually decreased in both arteries and veins. The collateral vessels were formed by dilation of originally existing capillaries. Capturing RBF changes around the onset of RVO is challenging and unrealistic in clinical practice; however, in our feline RVO model, we can begin observation even before inducing the occlusion. This feline RVO model may lead to further elucidation of the pathogenesis of RVO and may be helpful to understanding the pathological process in RVO.

Acknowledgments

The authors thank Enago (www.enago.jp) for the English language review.

Disclosure: **T. Wada**, None; **Y. Song**, None; **T. Oomae**, None; **K. Sogawa**, None; **T. Yoshioka**, None; **S. Nakabayashi**, None; **K. Takahashi**, None; **T. Tani**, None; **A. Ishibazawa**, None; **S. Ishiko**, None; **A. Yoshida**, None

References

1. Klein R, Klein BE, Moss SE, Meuer SM. The epidemiology of retinal vein occlusion: the Beaver Dam Eye Study. *Trans Am Ophthalmol Soc*. 2000;98:133–141; discussion 141-143.
2. Rogers S, McIntosh RL, Cheung N, et al. The prevalence of retinal vein occlusion: pooled data from population studies from the United States, Europe, Asia, and Australia. *Ophthalmology*. 2010;117:313–319.
3. Hayreh SS, Zimmerman MB, Podhajsky P. Incidence of various types of retinal vein occlusion and their recurrence and demographic characteristics. *Am J Ophthalmol*. 1994;117:429–441.
4. Jaulim A, Ahmed B, Khanam T, Chatziralli IP. Branch retinal vein occlusion: epidemiology, pathogenesis, risk factors, clinical features, diagnosis, and complications. An update of the literature. *Retina*. 2013;33:901–910.
5. Yuan A, Kaiser PK. Branch retinal vein occlusion. In: Ryan SJ (ed), *Retina*. London: Elsevier; 2013:1029–1038.
6. Rehak J, Rehak M. Branch retinal vein occlusion: pathogenesis, visual prognosis, and treatment modalities. *Curr Eye Res*. 2008;33:111–131.
7. Pournaras CJ, Rungger-Brandle E, Riva CE, Hardarson SH, Stefansson E. Regulation of retinal blood flow in health and disease. *Prog Retin Eye Res*. 2008;27:284–330.
8. Rosen DA, Marshall J, Kohner EM, Hamilton AM, Dollery CT. Experimental retinal branch vein occlusion in rhesus monkeys. II. Retinal blood flow studies. *Br J Ophthalmol*. 1979;63:388–392.
9. Avila CP, Jr, Bartsch DU, Bitner DG, et al. Retinal blood flow measurements in branch retinal vein occlusion using scanning laser Doppler flowmetry. *Am J Ophthalmol*. 1998;126:683–690.
10. Wang Y, Fawzi AA, Varma R, et al. Pilot study of optical coherence tomography measurement of retinal blood flow in retinal and optic nerve diseases. *Invest Ophthalmol Vis Sci*. 2011;52:840–845.
11. Suzuki N, Hirano Y, Yoshida M, et al. Microvascular abnormalities on optical coherence tomography angiography in macular edema associated with branch retinal vein occlusion. *Am J Ophthalmol*. 2016;161:126–132.
12. Coscas F, Glacet-Bernard A, Miere A, et al. Optical coherence tomography angiography in retinal vein occlusion: Evaluation of superficial and deep capillary plexa. *Am J Ophthalmol*. 2016;161:160–171.
13. Rispoli M, Savastano MC, Lumbroso B. Capillary network anomalies in branch retinal vein occlusion on optical coherence tomography angiography. *Retina*. 2015;35:2332–2338.
14. Khayat M, Lois N, Williams M, Stitt AW. Animal models of retinal vein occlusion. *Invest Ophthalmol Vis Sci*. 2017;58:6175–6192.
15. Ben-Nun J. Capillary blood flow in acute branch retinal vein occlusion. *Retina*. 2001;21:509–512.
16. Ameri H, Ratanapakorn T, Rao NA, Chader GJ, Humayun MS. Natural course of experimental retinal vein occlusion in rabbit; arterial occlusion following venous photothrombosis. *Graefes Arch Clin Exp Ophthalmol*. 2008;246:1429–1439.
17. Tani T, Song YS, Yoshioka T, et al. Repeatability and reproducibility of retinal blood flow measurement using a Doppler optical coherence tomography flowmeter in healthy subjects. *Invest Ophthalmol Vis Sci*. 2017;58:2891–2898.
18. Wang Y, Bower BA, Izatt JA, Tan O, Huang D. Retinal blood flow measurement by circumpapillary Fourier domain Doppler optical coherence tomography. *J Biomed Opt*. 2008;13:064003.
19. Leitgeb RA, Werkmeister RM, Blatter C, Schmetterer L. Doppler optical coherence tomography. *Prog Retin Eye Res*. 2014;41:26–43.
20. Spaide RF, Fujimoto JG, Waheed NK, Sadda SR, Staurenghi G. Optical coherence tomography angiography. *Prog Retin Eye Res*. 2018;64:1–55.
21. Nakabayashi S, Nagaoka T, Tani T, et al. Retinal arteriolar responses to acute severe elevation in systemic blood pressure in cats: role of endothelium-derived factors. *Exp Eye Res*. 2012;103:63–70.
22. Riva CE, Cranstoun SD, Mann RM, Barnes GE. Local choroidal blood flow in the cat by laser Doppler flowmetry. *Invest Ophthalmol Vis Sci*. 1994;35:608–618.
23. Attariwala R, Jensen PS, Glucksberg MR. The effect of acute experimental retinal vein occlusion on cat retinal vein pressures. *Invest Ophthalmol Vis Sci*. 1997;38:2742–2749.
24. Nagaoka T, Tani T, Song YS, et al. Evaluation of retinal circulation using segmental-scanning Doppler optical coherence tomography in anesthetized cats. *Invest Ophthalmol Vis Sci*. 2016;57:2936–2941.
25. Stanga PE, Tsamis E, Papayannis A, Stringa F, Cole T, Jalil A. Swept-Source Optical Coherence Tomography Angio (Topcon Corp, Japan): technology review. *Dev Ophthalmol*. 2016;56:13–17.
26. Munk MR, Giannakaki-Zimmermann H, Berger L, et al. OCT-angiography: a qualitative and quantitative comparison of 4 OCT-A devices. *PLoS One*. 2017;12:e0177059.
27. Christoffersen NL, Larsen M. Pathophysiology and hemodynamics of branch retinal vein occlusion. *Ophthalmology*. 1999;106:2054–2062.
28. Danis RP, Wallow IH. Microvascular changes in experimental branch retinal vein occlusion. *Ophthalmology*. 1987;94:1213–1221.
29. Fuma S, Nishinaka A, Inoue Y, et al. A pharmacological approach in newly established retinal vein occlusion model. *Sci Rep*. 2017;7:43509.

30. Nagaoka T, Sakamoto T, Mori F, et al. The effect of nitric oxide on retinal blood flow during hypoxia in cats. *Invest Ophthalmol Vis Sci*. 2002;43:3037–3044.
31. Noma H, Mimura T, Eguchi S. Association of inflammatory factors with macular edema in branch retinal vein occlusion. *JAMA Ophthalmol*. 2013;131:160–165.
32. Nagaoka T, Sogawa K, Yoshida A. Changes in retinal blood flow in patients with macular edema secondary to branch retinal vein occlusion before and after intravitreal injection of bevacizumab. *Retina*. 2014;34:2037–2043.